To be submitted to
Nuclear Instr. & Meth.

ISTITUTO NAZIONALE DI FISICA NUCLEARE
Laboratori Nazionali di Frascati

LNF-81/2(P)
9 Gennaio 1981

S. Bartalucci, R. Bertani, S. Bertolucci, M. Cordelli, R. Dini, P. Giromini, M. Pallotta, A. Rutili, A. Sermoneta and M. Spadoni: TEST OF A DRIFT CHAMBER WITH SECOND COORDINATE READOUT BY CHARGE DIVISION.

Servizio Documentazione
dei Laboratori Nazionali di Frascati
Cas. Postale 13 - Frascati (Roma)

INFN - Laboratori Nazionali di Frascati
Servizio Documentazione

LNF-81/2(P)
9 Gennaio 1981

TEST OF A DRIFT CHAMBER WITH SECOND COORDINATE READOUT BY CHARGE DIVISION.

S. Bartalucci, R. Bertani, S. Bertolucci, M. Cordelli, R. Dini, P. Giromini, M. Pallotta, A. Rutili, A. Sermoneta and M. Spadoni

INFN, Laboratori Nazionali di Frascati, and
INFN, Sezione di Pisa, S. Piero a Grado.

SUMMARY.

We have investigated the performances of a 1 metre long drift chamber prototype, where the second coordinate was also measured by using the charge division method. Positions were reconstructed with appreciable linearity in both drift and longitudinal directions. Particular attention has been devoted to the study of the position resolution attainable by charge division (3.2 mm FWHM in the chamber middle).

1. - INTRODUCTION.

In the design work of a magnetic detector dedicated to the study of e^+e^- reactions at low energies[1], we have tested a prototype of the central tracking system. Its drift chambers structure was chosen similar to that of the Mark II, Tasso and Cello detectors[2, 3, 4], but we exploited the possibility of deriving the longitudinal coordinate by the charge division method, and not by stereo view, in order to reduce the number of needed wire planes.

2. - CHAMBER DESCRIPTION.

The three cell prototype is sketched in Fig. 1. The chamber was filled with a mixture of 56% Argon and 44% ethane (it reaches[5] drift velocity saturation at relatively low fields ($\sim$ 600 V/cm)).

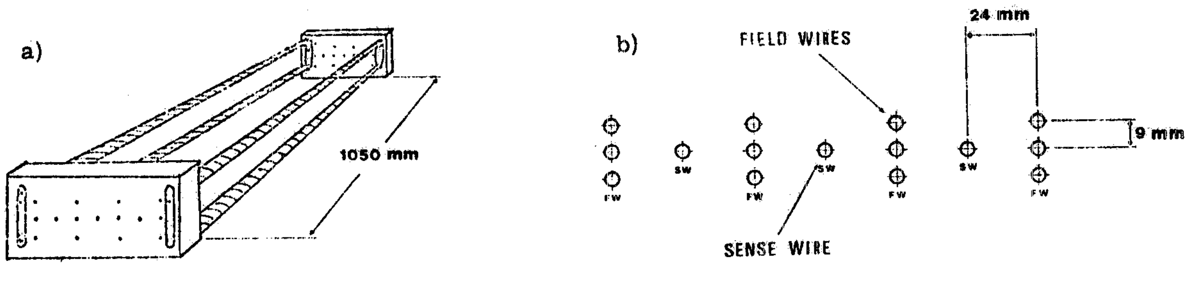

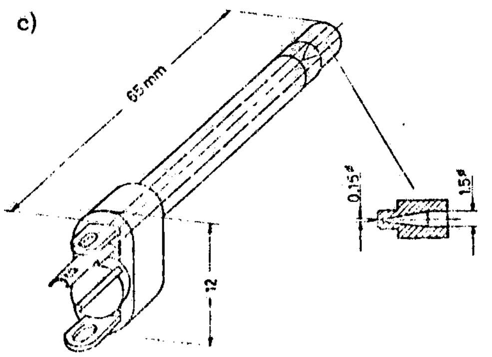

FIG. 1 - a) Chamber frame. It consists of two aluminum plates kept parallel by four machined rods.
b) Cell structure. Sense wires (30 μm stainless steel with resistivity 1826 Ω/m) and field wires (125 μm Cu-Be) are stret ched at 60 g and 400 g respectively.
c) Delrin wire feedthroughs. They keep wires in position once inserted into preci sion holes drilled through the aluminum plates.

The shape and the strength of the electric field was carefully studied as a function of the wires voltages, diameters and geometry. Field lines, for the final geometry and for a typical voltages setting used during the tests, are shown in Fig. 2.

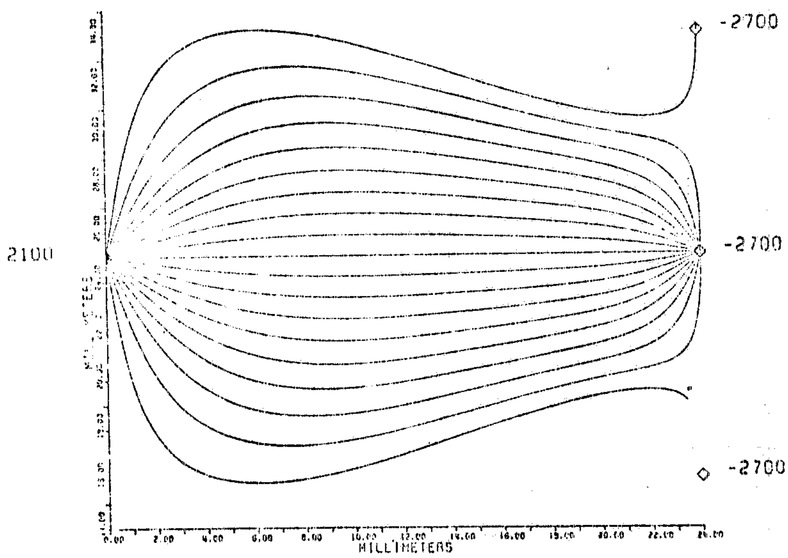

FIG. 2 - Field lines for the adopted cell (half cell shown). The sense wire is at 2100 V, field wires are at - 2700 V. Along the straight field line conecting the sense and the central field wire and in re gion of $\pm$5 mm around it, the electric field always ex ceeds 700 V/cm.

A detailed analysis[6,7,8] of the charge division method shows that the value R of the wire resistance should be high in order to keep low the noise and to improve the position resolution along the wire. On the other hand a small R value is required in order to have high resolution in the drift time measurement and good linearity in the position determination by charge division. The best compromise is achieved by putting $R = 2\pi\sqrt{\frac{L}{C}}$. In our case ($C \simeq 10$ pF, $L \simeq 1.3$ μH), R = 2.3 KΩ should be used. We found available a 30 μ stainless steel wire (resistivity 1826 KΩ/m) so that, in our prototype, we had R $\sim$ 2.1 KΩ.

The dedicated home-made electronics consisted of an amplifier-discriminator (Fig. 3) for drift time measurements and of low input impedence amplifiers (Fig. 4) for the charge division.

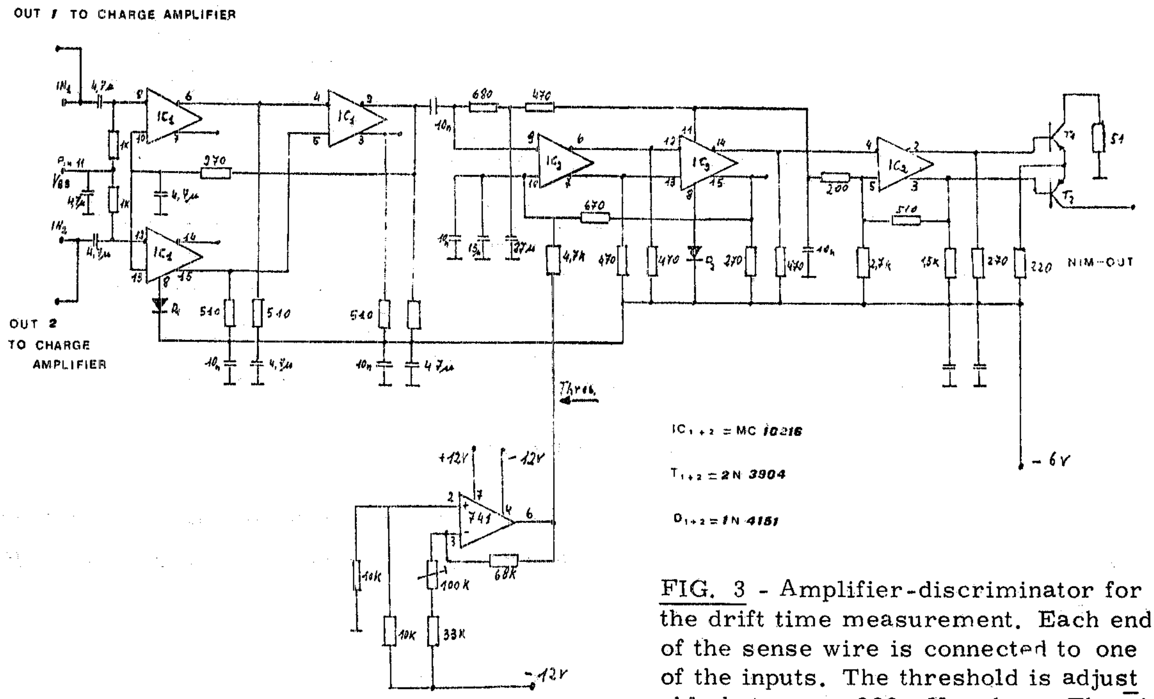

FIG. 3 - Amplifier-discriminator for the drift time measurement. Each end of the sense wire is connected to one of the inputs. The threshold is adjustable between -200 μV and ∞. The risetime is about 2 ns and the time slewing $\leq$ 1 ns for input amplitudes 110 % of the threshold and above.

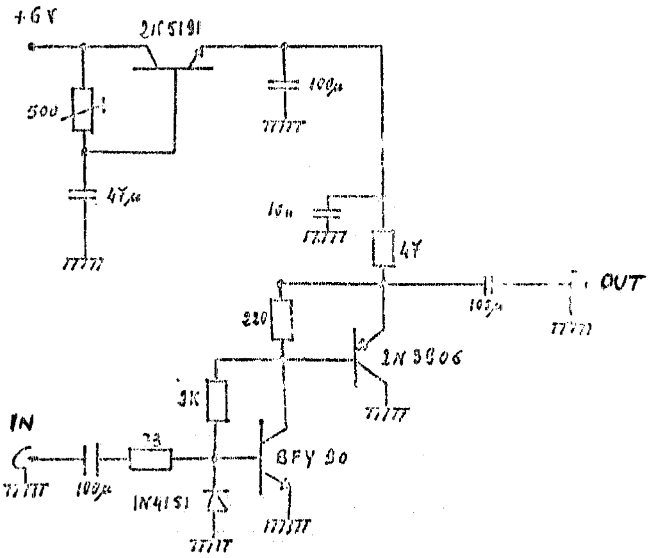

FIG. 4 - The amplifier for charge division. The gain is 32 and the risetime about 25 ns. One amplifier is needed for each wire end.

3. - CHAMBER PERFORMANCE.

The chamber has been tested with a collimated Ru^{106} source. Decay electrons were defined in space and time by a three scintillation counters telescope. The electronics flow chart is shown in Fig. 5.

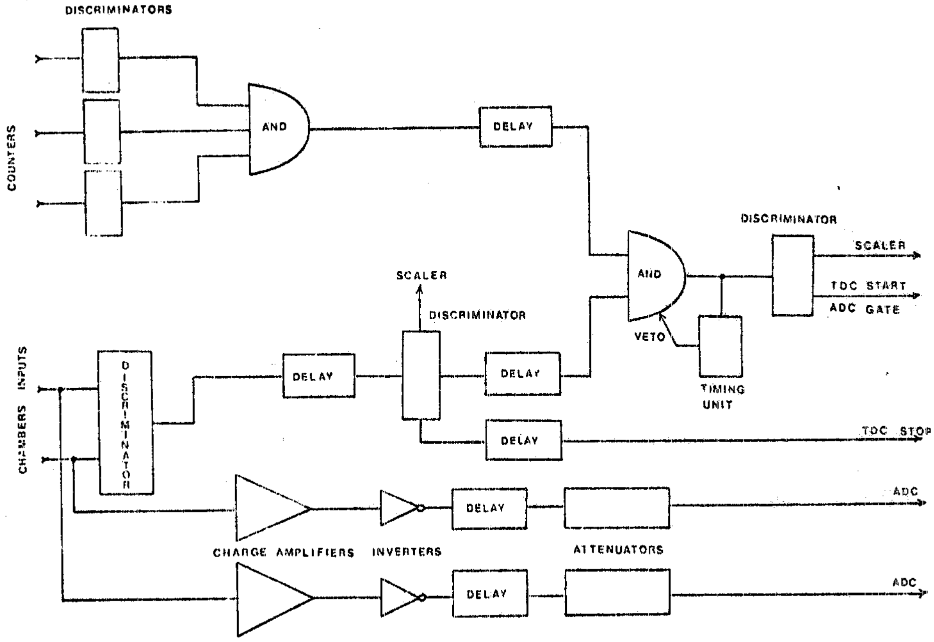

FIG. 5 - Flow diagram of the electronics.

The chamber efficiency has been measured as a function of the sense and field wires voltages at several relevant positions. Always the chamber shows a long plateau curve, with efficiency $\approx$ 99 % (Fig. 6).

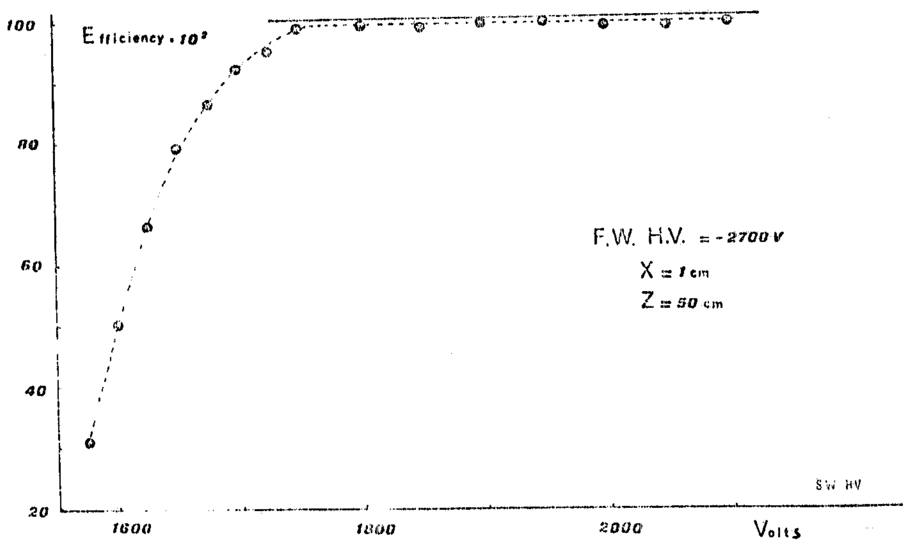

FIG. 6 - Efficiency of the chamber as a function of the sense wire H. V., z is the longitudinal coordinate, x is the coordinate transverse to the sense wire (x = 0).

Drift time measurements have been performed by moving the chamber in the direction perpendicular to the sense wire (x) over the whole cell length and for several longitudinal positions. At each position the peak of the T.O.F. distribution has been recorded (see Fig. 7). The drift velocity was determined to be 51.3 ± 0.7 mm/μs in good agreement with previous measurements[5].

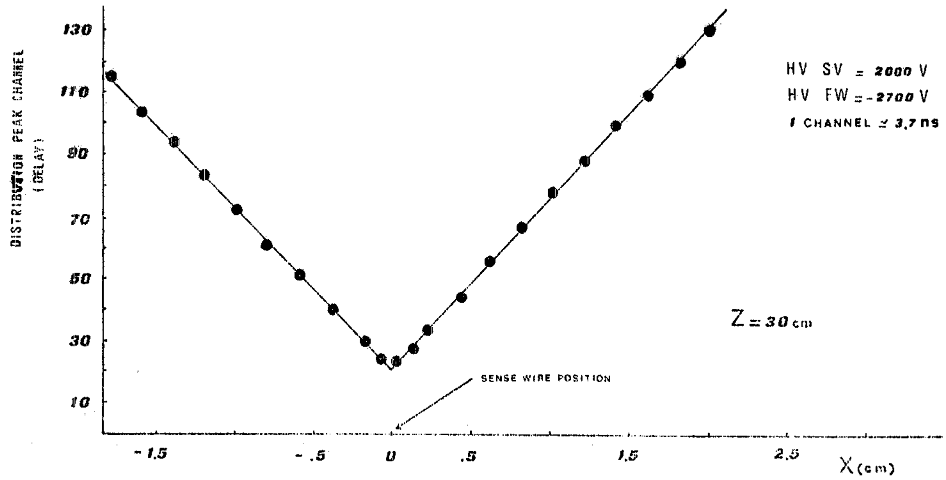

FIG. 7 - The measured drift time as a function of the Ru^{106} source distance x from the sense wire. Analogous sets of measurements were repeated along the wire in step of 10 cm.

The chamber has been also scanned longitudinally at several fixed x positions. Signals from both sense wire ends (A and B) have been recorded, after integrating over 180 nsec, and off-line corrected for slight amplificator differences and for ADC non linearities. Fig. 8 shows the measured distributions of the ratio A/A+B when moving the Ru^{106} source parallel to the sense wire. Distribution peaks vs. source position are shown in Fig. 9.

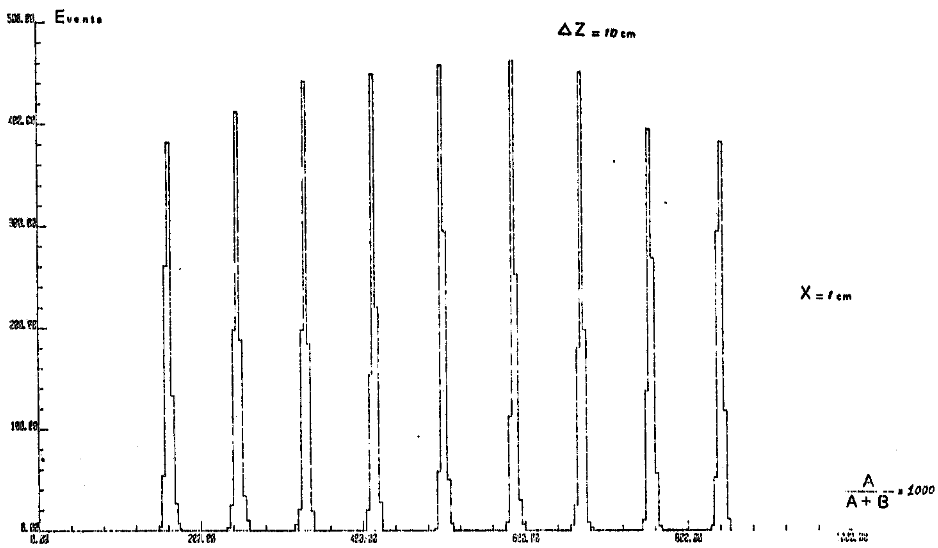

FIG. 8 - Set of Ru^{106} position distributions obtained displacing the chamber along the sense wire in steps of 10 cm.

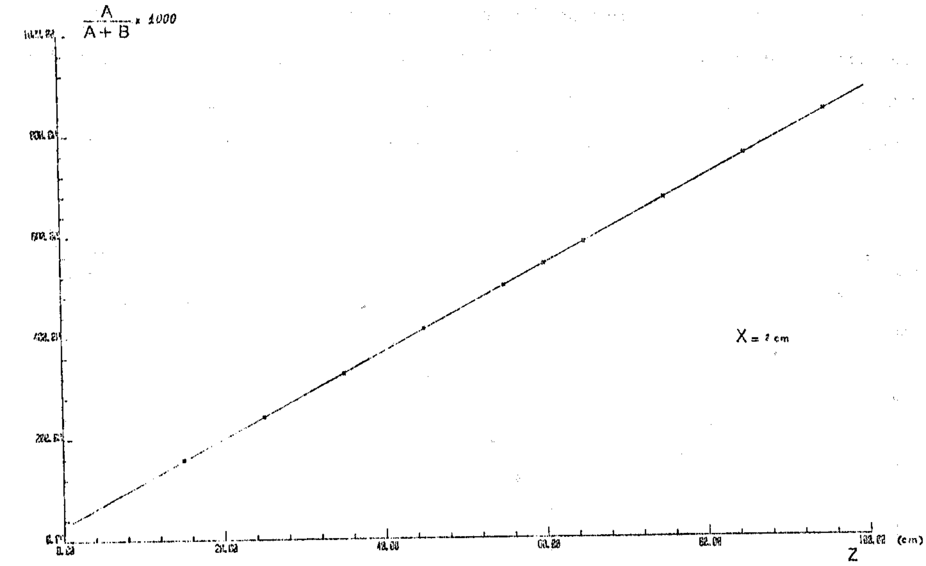

FIG. 9 - ⟨A/A+B⟩ as a function of the source positron z along the sense wire. A/A+B is the ratio of the charge flowing out of one end of the resistive line and the total charge from both ends.

The position resolution value and its dependence on the position along the wire have been studied by gaussian-fitting the measured distributions. Contributions of the source dimensions were monitored by the drift coordinate measurement. A T.O.F. distribution, yielding a source width of 5.3 mm FWHM, is shown in Fig. 10.

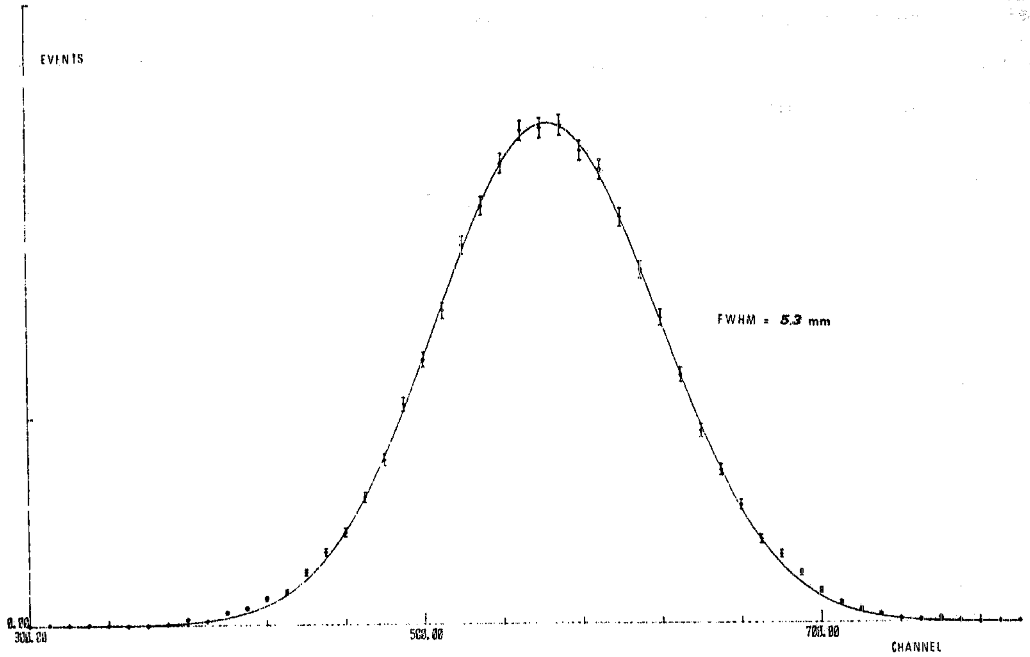

FIG. 10 - Source profile along the x axis as given by the drift time measurement (its resolution is estimated ≤ 0.2 mm). The same yield was assumed for the source distribution along the z axis.

Fig. 11 shows the resolution behaviour along the wire, with and without source subtraction. The resolution is $\sim$3.2 mm FWHM (i. e. 0.27% of the wire length) at the approximate center of the chamber and deteriorates, moving toward both ends, up to 7.1 mm FWHM (0.62%).

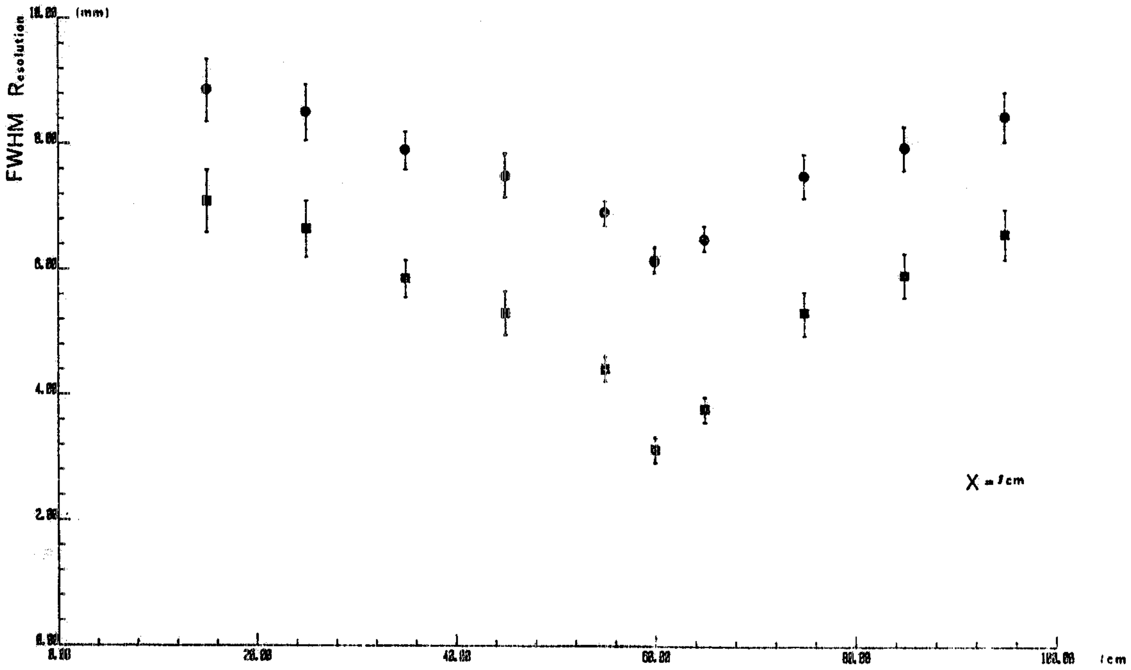

FIG. 11 - Resolution at different z positions as obtained from gaussian fits to the measured distributions (points). Square indicate the resolutions obtained by subtracting the source contribution.

ACKNOWLEDGMENTS.

We gratefully acknowledge the help of Dr. U. Kötz, for many useful discussions and for providing us with the wire feedthroughs used to build the prototype. Mrs. A. Ruperti, M. Favati and L. Giacomelli provided skillful technical help during the prototype construction.

REFERENCES.

(1) - M. Bassetti, M. Biagini, R. Boni, V. Chiarella, V. Chimenti, E. Fiorentino, S. Guiducci, G. Martinelli, M. Preger, C. Sanelli, M. Serio, S. Tazzari, F. Tazzioli, S. Bartalucci, S. Bertolucci, R. Del Fabbro, P. Giromini, E. Iarocci, C. Moriggi, G. P. Murtas, G. Piano Mortari, A. Sermoneta, M. Spinetti, L. Trasatti, M. Ambrosio, G. Barbarino, G. Paternoster, S. Patricelli, U. Troya, G. Bellettini, C. Cerri, F. Sergiampietri, M. Spadoni and F. Zetti, Frascati Internal Report LNF-77/3(int.) (1977).

(2) - W. Davies-White, G. E Fischer, M. J. Lateur, R. H. Schindler, R. F Schwitters, J. L. Siegrist, H. Taureg, H. Zaccone and D. L. Hartill, Nuclear Instr. and Meth. 160, 227 (1979).

(3) - H. Boerner, H. M. Fischer, H. Hartmann, B. Lohr, M. Wollstadt, D. G. Cassel, U. Kotz, H. Kowalski, B. H. Wiik, R. Fohrmann and P. Schmuser, DESY Report 80/27 (1980).

(4) - W. DeBoer, B. Budjarek, W. Fues, G. Grindhammer, R. Kotthaus, H. Lierl and L. Moss, Nuclear Instr. and Meth. 156, 249 (1978).

(5) - H. Daum, C. W Fabjan, S. H. Pordes, M. Franklin, P. Dam and A. F. Rothenberg, Nuclear Instr. and Meth. 152, 541 (1978).

(6) - V. Radeka, IEEE Trans. Nucl. Sci. NS-21, 51 (1974).

(7) - J. L. Alberi and V. Radeka, IEEE Trans. Nucl. Sci. NS-23, n. 1 (1974).

(8) - V. Radeka and P. Rehak, IEEE Trans. Nucl. Sci. NS-25, n. 1 (1978).